Evaluation of Hyperspectral Reflectance Indexes to Detect Grapevine Water Status in Vineyards

José R. Rodríguez-Pérez,[1] David Riaño,[2] Eli Carlisle,[3] Susan Ustin,[2] and David R. Smart[3]*

Abstract: Irrigation scheduling is critical as it affects both fruit yield and composition. We examined the potential to use field-measured hyperspectral remote sensing data (reflectance and transmission over the 350–2500 nm wavelength region) to estimate leaf water content, equivalent water thickness (EWT), and leaf water potential (Ψ) in a commercial vineyard of *Vitis vinifera* cv. Pinot noir. The data allowed us to evaluate a number of reflectance patterns to estimate vine water status through correlations using two spectral approaches: direct measurement of vegetation indexes (VIs) and continuum removal analysis (CRA). Continuum removal analysis was applied to obtain the maximum band depth (MBD) and the band area (BA) of several absorption features sensitive to water content. Correlations were high for EWT at the leaf level using a modification of the Simple Ratio VI (SR2; $R^2 = 0.916$) and for CRA with MBD_{970} ($R^2 = 0.917$) and BA_{1160} ($R^2 = 0.897$). Correlations with EWT and water potential at the canopy level for SR2 were nonsignificant, which was characteristic for many VIs. For predawn water potential (Ψ_{PD}) and midday stem water potential (Ψ_{stem}) at the canopy level, best fits were realized for Modified Triangular VI (MTVI2; $R^2 = 0.360$) and Red/Green VI (RGI, R_{695}/R_{554}; $R^2 = 0.462$), respectively. For canopy level water status, the best results were obtained using the difference between the midday stem water potential and the predawn leaf water potential ($\Psi_{stem} - \Psi_{PD}$) with $R^2 = 0.619$ for RGI and $R^2 = 0.541$ for Structure Intensive Pigment Index (SIPI, $R_{800}-R_{445}/R_{800}-R_{680}$), while for CRA $R^2 = 0.477$ for BA_{1600} and $R^2 = 0.509$ for MBD_{970}. Results suggest that noninvasive monitoring using hyperspectral data could improve current methods for estimating water status in individual vines. Applications of similar measurements could be produced from airborne hyperspectral imagers to provide spatially resolved estimates of water stress for use in water management of large-scale commercial vineyards.

Key words: vineyard remote sensing, vine water stress, leaf reflectance, canopy reflectance, vegetation index

Abbreviations: Ψ_{leaf}, midday leaf water potential (MPa); Ψ_{PD}, predawn leaf water potential (MPa); Ψ_{stem}, midday stem water potential (MPa); Ψ_{s}, osmotic potential (MPa); Ψ_{t}, turgor pressure (MPa); g_{s}, stomatal conductance to water vapor (mmol m^{-2} s^{-1}); E, transpiration rate (mmol H$_2$O m^{-2} s^{-1}); A, net photosynthetic rate (µmol CO$_2$ m^{-2} s^{-1}); LA, leaf area (cm^2); LAI, leaf area index (m^2 m^{-2}); Wt, total leaf weight (g); Wd: oven dry leaf weight (g); RWC, relative water content (%); WCd, water content as percent of dry mass (%); WCt, water content as percent of total fresh mass (%); EWT, equivalent water thickness (g cm^{-2}); SLW, specific leaf weight dry mass (kg m^{-2}); TSLW, total specific leaf fresh weight (kg m^{-2}); CRA, continuum removal analysis; BA, band area of the absorption feature in CRA; D, band depth in CRA; R, measured reflectance; MBD, maximum band depth of the absorption feature in CRA; lMBD, wavelength of the maximum band depth of the absorption feature in CRA (nm); FWHM, full band width at half maximum (nm); REIP, red-edge inflection position (nm); REIPv, derivative value of REIP (nm); ASD, Analytical Spectral Device (350–2500 nm); VIS, visual light spectrum (400–700 nm); IR, infrared light (750 nm–1 mm); NIR, near-IR (700–1300 nm); MIR, mid-IR (1300–2500 nm); SWIR, shortwave IR reflectance (1400–3000 nm); Rs, reflectance (relative units); Is, leaf reflectance (relative units); Id, leaf reflectance in the dark (relative units); Ir reference reflectance (relative units); VI, vegetation index(es) (waveband ratios)

[1]Universidad de León, Área de Ingeniería Cartográfica, Geodésica y Fotogrametría, Avda. de Astorga, s/n, 24400 Ponferrada León, Spain; [2]Center for Spatial Technologies and Remote Sensing and [3]Department of Viticulture and Enology, University of California, Davis, CA 95616.

*Corresponding author (email: drsmart@ucdavis.edu)

Water stress conditions the quality of many crops, including winegrapes (Kennedy et al. 2002). Several physiological indicators are used to assess plant water status, or stress, with stomatal conductance (g_{s}), leaf water potential (Ψ_{leaf}), and transpiration rate (E) the most widely used in viticulture. These physiological stress indicators are strongly related to factors such as relative water content (RWC; leaf water content divided by its content at full turgor), osmotic potential (Ψ_{s}), turgor pressure (Ψ_{t}), and net photosynthetic rates (A), most of which have been commonly used to ground verify remotely sensed measures of plant water stress (Peñuelas et al. 1993, Serrano et al. 2000, Cifre et al. 2005, Stimson et al. 2005). Predawn leaf water potential (Ψ_{PD}) approximates to the soil water

potential and can also serve as an indicator of stress (Donovan et al. 1999), while midday leaf (Ψ_{leaf}) and stem (Ψ_{stem}) water potential (McCutchan and Shackel 1992) provide measures of water status under high evapotranspiration demand. Both midday water potential measurements of Ψ_{leaf} and Ψ_{stem} are highly correlated (Williams and Araujo 2002). In this study we used Ψ_{stem} because it has lower variation within individual vine canopies compared with Ψ_{leaf} (D.R. Smart, 2006 unpublished data).

Measuring the water status of leaves or shoots is time consuming and subject to measurement and sampling errors, especially when data are extrapolated to the whole plant or to the vineyard scale. It can also be difficult to compare studies using Ψ_{stem} or Ψ_{leaf} because of differences in operational procedures. Measurement of leaf reflectance may provide a better approach to standardize water status measurements for specific grapevine varieties. The spectral signature of vegetation is distinctive and characterized by low reflectance in the visible region (VIS: 400–700 nm), high reflectance in near-infrared region (NIR; 700–1300 nm), and intermediate reflectance in the short-wave infrared (SWIR; 1400–3000 nm). Variation of NIR reflectance is independent of water content, but variation in SWIR wavelengths is strongly affected by water. The viewing of indicators that combine these spectral regions allows vegetation to be classified and different vegetation properties to be determined.

Reflectance depends in part on the water stored in the leaf cells, especially for NIR and mid-infrared (MIR; 1300–2500 nm) wavelengths (Hunt and Rock 1989, Hunt et al. 1987, Gao 1996, Ceccato et al. 2001). For wavelengths sensitive to water absorption (760, 970, 1450, 1940, and 2950 nm), leaf and canopy reflectance decreases with increasing tissue water content (Bowman 1989, Hunt et al. 1987, Gao 1996, Peñuelas et al. 1997a, Ripple 1986). These wavelength "bands" can be combined in numerous ways to generate vegetation indexes (VIs) related to water status (Hunt and Rock 1989, Carter 1994, Mogensen et al. 1996, Bahrun et al. 2003). Some authors have used VIs to estimate crop water status (Peñuelas et al. 1993, 1997a, Mogensen et al. 1996, Jones et al. 2004) and several have been proposed in remote sensing studies (Broge and Leblanc 2001, Broge and Mortensen 2002, Zarco-Tejada et al. 2005a,b). Thus, remote sensing may provide a nondestructive, rapid, and reliable method for assessing water status (Hunt et al. 1987, Hunt and Rock 1989, Li et al. 2005), and, from airborne and satellite imagers, provide 100% sampling or viewing of a vineyard. Three major water absorption regions have been identified that produced the best overall correlations with water content: 950–970, 1150–1260, and 1520–1540 nm (Sims and Gamon 2003). These bandwidths were used in this investigation. The spectral bands used in some VIs in this study were changed from their original definition by slightly decreasing the spectral bandwidths (as specified in Table 1) to more accurately reflect those showing the best overall correlations.

Vegetation water content can be related in general to spectral reflectance measurements using two indicators: the equivalent water thickness (EWT), or the ratio of the mass of water to the leaf area (Danson et al. 1992, Ceccato et al. 2001), and the ratio between the mass of leaf water and either the fresh weight (Mbow 1999) or the dry weight (Chuvieco et al. 2002). Several researchers have used Ψ_{leaf} to provide ground verification of remotely sensed water status (Peñuelas et al. 1997a, Flexas et al. 2000, Jones et al. 2004, Dobrowski et al. 2005), but have not always reported correlations of Ψ_{leaf} with their remotely sensed data. An early investigation did find high correlations between Ψ_{leaf} and MIR reflectance that were attributed to covariance with the RWC and leaf cover (Ripple 1986). Significant relationships have been demonstrated between Ψ_{leaf} and reflectance ratios, multivariate and derivative reflectance indexes for sunflower (*Helianthus annuus* L.), with R^2 values from 0.30 to -0.74 (Peñuelas et al. 1994). More recently, a strong correlation was demonstrated between several VIs and Ψ_{leaf} for drought-stressed conifers in the southwest (Stimson et al. 2005).

Remote sensing indicators are hindered by several factors in estimating water status. Leaf structure, for example, influences the depth of water absorption bands (Danson et al. 1992). Taking the derivative of the reflectance at wavelengths corresponding to the edges of the water absorption bands can minimize interference from leaf structure and maximize sensitivity to leaf water content (Danson et al. 1992, Zarco-Tejada et al. 2003). Furthermore, chronic water stress and low water content can be detected as a consequence of loss of chlorophyll; however, it is a cumulative symptom of water stress, and thus does not provide early monitoring for management. The influence of background materials on the water absorption bands causes a further detection problem, which can be managed with continuum removal analysis (CRA) (Kokaly and Clark 1999). The continuum is the "background absorption" (Clark 1999); that is, an estimate of absorption by the background materials at a specific absorption feature of interest. This analysis establishes a relationship between an absorption feature of interest (e.g., leaf water content) and maximum band depth (MBD) and band area (BA) under the continuum (Curran et al. 2001, Kokaly et al. 2003, Huang et al. 2004). The maximum band depth position (λMBD) and the full width of the feature at half maximum (FWHM) have also shown promise as indicators of reflectance anomalies (Fischer et al. 2003).

This study tested the utility of several vegetative indexes to detect vine water content and relate those indexes to water status (Table 1). We made several direct measures of vine water status, including Ψ_{stem}, Ψ_{PD}, EWT, water content as percent of dry mass (WCd), and water content as percent of total fresh mass (WCt). The investigation was carried out in a Pinot noir vineyard with extreme spatial heterogeneity in soil available water, and we evaluated the ability to detect water status under natural field conditions using numerous reflectance measurements:

Table 1 Vegetation indexes (VI) at specific reflectance wavelengths (R_i) tested in this study.

Index (abbreviation)	Equation	Reference
Greenness (GI)	$GI = \dfrac{R_{554}}{R_{677}}$	Zarco-Tejada et al. 2005a, 2005b
Zarco-Tejada and Miller (ZTM)	$ZM = \dfrac{R_{750}}{R_{710}}$	Zarco-Tejada et al. 2001, 2005a
Red/Green (RGI)	$RGI = \dfrac{R_{695}}{R_{554}}$	after Fuentes et al. 2001, Gamon and Surfus 1999
Red/Green (RGI1)	$RGI1 = \dfrac{R_{690}}{R_{550}}$	Zarco-Tejada et al. 2005a,b
Blue/Green (BGI)	$BGI = \dfrac{R_{400}}{R_{550}}$	after Zarco-Tejada et al. 2005a,b
Blue/Green (BGI1)	$BGI1 = \dfrac{R_{420}}{R_{554}}$	after Zarco-Tejada et al. 2005a,b
Blue/Green (BGI2)	$BGI2 = \dfrac{R_{400}}{R_{550}}$	Zarco-Tejada et al. 2005a,b
Blue/Red (BRI)	$BRI = \dfrac{R_{400}}{R_{690}}$	Zarco-Tejada et al. 2005a,b
Blue/Red (BRI1)	$BRI1 = \dfrac{R_{450}}{R_{690}}$	Zarco-Tejada et al. 2005a,b
Blue/Red (BRI2)	$BRI2 = \dfrac{R_{440}}{R_{690}}$	This study
Ratio Vegetation (RVI)	$RVI = \dfrac{R_{800}}{R_{673}}$	after Broge and Mortensen 2002
Green/Red Ratio (GRR)	$GRR = \dfrac{R_{554}}{R_{673}}$	Fuentes et al. 2001
Normalized Green/Red Ratio (NGRR)	$NGRR = \dfrac{R_{673} - R_{554}}{R_{673} + R_{554}}$	This study
Normalized Green/Red Ratio (NGRR1)	$NGRR_1 = \dfrac{R_{673} + R_{554}}{R_{673} - R_{554}}$	This study
Simple Ratio (SR1)	$SR = \dfrac{R_{845}}{R_{665}}$	after Broge and Mortensen 2002
Simple Ratio (SR1)	$SR1 = \dfrac{R_{695}}{R_{760}}$	This study
Simple Ratio (SR2)	$SR2 = \dfrac{R_{1070}}{R_{1340}}$	This study
Simple Ratio (SR3)	$SR3 = \dfrac{R_{678}}{R_{880}}$	This study
Simple Ratio (SR4)	$SR4 = \dfrac{R_{678}}{R_{1070}}$	This study
Red/Blue (RBI)	$RBI = \dfrac{R_{695}}{R_{445}}$	This study
Difference Vegetation (DVI)	$DVI = R_{880} - R_{673}$	after Broge and Mortensen 2002
Moisture Stress (MSI)	$MSI = \dfrac{R_{1650}}{R_{835}}$	after Hunt and Rock 1989
Moisture Stress (MSI1)	$MSI1 = \dfrac{R_{870}}{R_{1350}}$	This study
Normalized Difference VI (NDVI)	$NDVI = \dfrac{R_{845} - R_{665}}{R_{845} + R_{665}}$	after Rouse et al. 1974
Normalized Difference VI (NDVI1)	$NDVI1 = \dfrac{R_{880} - R_{673}}{R_{880} + R_{673}}$	Zhao et al. 2005
Normalized Difference VI (NDVI2)	$NDVI2 = \dfrac{R_{858.5} - R_{645}}{R_{858.5} + R_{645}}$	This study
Normalized Difference VI (NDVI3)	$NDVI3 = \dfrac{R_{870} - R_{673}}{R_{870} - R_{673}}$	This study

Index (abbreviation)	Equation	Reference
Normalized Difference Vegetation (NDVI4)	$NDVI4 = \dfrac{R_{884} - R_{680}}{R_{884} + R_{680}}$	This study
Modified NDVI (mNDVI)	$mNDVI = \dfrac{R_{750} - R_{705}}{R_{750} + R_{705}}$	Fuentes et al. 2001, Gitelson et al. 1996
Photochemical Reflectance (PRI)	$PRI = \dfrac{R_{531} - R_{570}}{R_{531} + R_{570}}$	Fuentes et al. 2001, Gamon and Surfus 1999
Photochemical Reflectance (PRI1)	$PRI1 = \dfrac{R_{528} - R_{567}}{R_{528} + R_{567}}$	after Gamon et al. 1992
Photochemical Reflectance (PRI2)	$PRI2 = \dfrac{R_{531} - R_{570}}{R_{531} + R_{570}}$	after Gamon et al. 1992, Peñuelas et al. 1997b
Photochemical Reflectance (PRI3)	$PRI3 = \dfrac{R_{570} - R_{539}}{R_{570} + R_{539}}$	after Gamon et al. 1992
Normalized Pigments Chlorophyll Ratio (NPCI)	$NPCI = \dfrac{R_{680} - R_{430}}{R_{680} + R_{430}}$	Peñuelas et al. 1994
Simple Ratio Pigment (SRPI)	$SRPI = \dfrac{R_{430}}{R_{680}}$	Peñuelas et al. 1995a
Normalized Phaeophytinization (NPQI)	$NPQI = \dfrac{R_{415} - R_{435}}{R_{415} + R_{435}}$	Barnes 1992; Peñuelas et al. 1995a
Structure Intensive Pigment (SIPI)	$SIPI = \dfrac{R_{800} - R_{445}}{R_{800} + R_{680}}$	after Peñuelas et al. 1995b, Zarco-Tejada et al. 2005a
Structure Intensive Pigment (SIPI1)	$SIPI1 = \dfrac{R_{800} - R_{450}}{R_{800} + R_{650}}$	after Peñuelas et al. 1995b, Zarco-Tejada et al. 2005a
Normalized Difference Nitrogen (NDNI)	$NDNI = \dfrac{\log(1/R_{1510}) - \log(1/R_{1680})}{\log(1/R_{1510}) + \log(1/R_{1680})}$	Serrano et al. 2002
Normalized Difference Lignin (NDLI)	$NDLI = \dfrac{\log(1/R_{1754}) - \log(1/R_{1680})}{\log(1/R_{1754}) + \log(1/R_{1680})}$	Serrano et al. 2002
Cellulose Absorption (CAI)	$CAI = 0.5*(R_{2000} + R_{2200}) - R_{2100}$	Nagler et al. 2000
Normalized Difference Water (NDWI)	$NDWI = \dfrac{R_{860} - R_{1240}}{R_{860} + R_{1240}}$	Gao 1996, Zarco-Tejada et al. 2003
Normalized Difference Water (NDWI1)	$NDWI1 = \dfrac{R_{858.5} - R_{1240}}{R_{858.5} - R_{1240}}$	Gao 1996
Normalized Difference Water (NDWI2)	$NDWI2 = \dfrac{R_{870} - R_{1260}}{R_{870} + R_{1260}}$	This study
Water Band (WBI)	$WBI = \dfrac{R_{970}}{R_{900}}$	Peñuelas et al. 1993
Water (WI)	$WI = \dfrac{R_{900}}{R_{970}}$	Peñuelas et al. 1997a
Floating Position Water Band (fWBI)	$fWBI = \dfrac{R_{900}}{\min(R_{930\text{-}980})}$	Strachan et al. 2002
Simple Ratio Water (SRWI)	$SRWI = \dfrac{R_{858}}{R_{1240}}$	Zarco-Tejada et al. 2003
Simple Ratio Water (SRWI1)	$SRWI1 = \dfrac{R_{880}}{R_{1265}}$	This study
Simple Ratio Water (SRWI2)	$SRWI2 = \dfrac{R_{1350}}{R_{870}}$	This study
Simple Ratio Water (SRWI3)	$SRWI3 = \dfrac{R_{880}}{R_{1265}}$	This study
Transformed Chlorophyll Absorption in Reflectance (TCARI)	$TCARI = 3*[(R_{700} - R_{670}) - 0.2*(R_{700} - R_{550})]*(R_{700}/R_{670})$	Haboudane et al. 2002
Modified Chlorophyll Absorption in Reflectance (MCARI)	$MCARI = [(R_{700} - R_{670}) - 0.2*(R_{700} - R_{550})]*(R_{700}/R_{670})$	Daughtry et al. 2000
Modified Chlorophyll Absorption in Reflectance (MCARI1)	$MCARI_1 = 1.2*[2.5*(R_{800} - R_{670}) - 1.3*(R_{800} - R_{550})]$	Haboudane et al. 2004

Index (abbreviation)	Equation	Reference
Modified Chlorophyll Absorption in Reflectance (MCARI2)	$MCARI_2 = \dfrac{1.5*[2.5*(R_{800}-R_{670})-1.3*(R_{800}-R_{550})]}{\sqrt{(2*R_{800}+1)^2-(6*R_{800}-5*R_{670})-0.5}}$	Haboudane et al. 2004
Modified triangular VI (MTVI1)	$MTVI3 = 1.2*[1.2*(R_{800}-R_{550})-2.5*(R_{670}-R_{550})]$	Haboudane et al. 2004
Modified triangular VI (MTVI2)	$MTVI2 = \dfrac{1.5*[1.2*(R_{800}-R_{550})-2.5*(R_{670}-R_{550})]}{\sqrt{(2*R_{800}+1)^2-(6*R_{800}-5*R_{670})-0.5}}$	Haboudane et al. 2004
Modified triangular VI (MTVI3)	$MTVI3 = 1.2*[1.2*(R_{880}-R_{554})-2.5*(R_{758}-R_{554})]$	This study
Renormalized Difference VI (RDVI)	$RDVI = \sqrt{\dfrac{R_{880}-R_{673}}{R_{880}+R_{673}}*(R_{880}-R_{673})}$	Reujean and Breon 1995
Modified Simple Ratio (MSR)	$MSR = \dfrac{R_{845}/R_{665}-1}{(R_{845}/R_{665})^{0.5}+1}$	after Chen 1996
Triangular VI (TVI)	$TVI = 0.5*[120*(R_{750}-R_{550})-200*(R_{670}-R_{550})]$	Broge and Leblanc 2001
Triangular VI (TVI1)	$TVI1 = 0.5*[120*(R_{758}-R_{554})-200*(R_{674}-R_{554})]$	This study
Carter (Crt1)	$Crt1 = \dfrac{R_{695}}{R_{420}}$	Carter 1994
Carter (Crt2)	$Crt2 = \dfrac{R_{695}}{R_{760}}$	Carter et al. 1996
Carter (Crt3)	$Crt3 = \dfrac{R_{700}}{R_{420}}$	This study
Lichtenthaler (Lic)	$Lic = \dfrac{R_{800}-R_{680}}{R_{800}+R_{680}}$	Lichtenthaler et al. 1996
Lichtenthaler (Lic1)	$Lic1 = \dfrac{R_{440}}{R_{690}}$	Lichtenthaler et al. 1996
Lichtenthaler (Lic2)	$Lic2 = \dfrac{R_{440}}{R_{740}}$	Lichtenthaler et al. 1996
Vogelmann (Vog)	$Vog = \dfrac{R_{740}}{R_{720}}$	Vogelmann 1993, Zarco-Tejada et al. 1999
Vogelmann (Vog1)	$Vog1 = \dfrac{R_{734}-R_{747}}{R_{715}+R_{726}}$	Vogelmann 1993, Zarco-Tejada et al. 1999
Vogelmann (Vog2)	$Vog2 = \dfrac{R_{734}-R_{747}}{R_{715}+R_{720}}$	Vogelmann 1993, Zarco-Tejada et al. 1999
Gitelson and Merzlyak (GM1)	$GM1 = \dfrac{R_{750}}{R_{550}}$	Gitelson and Merzlyak 1997
Gitelson and Merzlyak (GM2)	$GM2 = \dfrac{R_{750}}{R_{700}}$	Gitelson and Merzlyak 1997
Curvature (CUR)	$CUR = \dfrac{R_{675}*R_{690}}{R_{683}^2}$	Zarco-Tejada et al. 2000
Normalized Difference IR (NDII)	$NDII = \dfrac{R_{835}-R_{1650}}{R_{835}-R_{1650}}$	Hardisky et al. 1983; van Niel 2003
Chlorophyll Absorption Ratio (CARI)	$CARI = CAR\dfrac{R_{700}}{R_{670}}$	Kim et al. 1994, Broge and Leblanc 2001
Enhanced VI (EVI)	$EVI = 2.5*\dfrac{R_{858.5}-R_{645}}{R_{858.5}+6*R_{645}-7.5*-R_{469}+1}$	Huete et al. 2002
Shortwave Infrared Water Stress (SIWSI)	$SIWSI = \dfrac{R_{858.5}-R_{1640}}{R_{858.5}+R_{1640}}$	Fensholt and Sandholt 2003
Chlorophyll Absorption Ratio (CAR)	$CAR = \dfrac{a*670+R_{670}+b}{\sqrt{a^2+1}}; a = R_{700}-R_{550}; b = R_{550}-(a*550)$	Broge and Leblanc 2001

VIs and VIs derived using CRA. The CRA parameters were red-edge inflection position (REIP, nm) and its derivative (REIPv), MBD and lMBD, BA, and FWHM, all calculated for different wavelength intervals. The analysis was carried out at leaf and canopy levels to provide a more complete assessment of methods that might be directly applicable to commercial vineyard management.

Materials and Methods

Study site. The vineyard was located in the Carneros region, Napa Valley, CA, and owned by the Robert Mondavi Corporation at the time of the investigation and has the following coordinate boundaries: SW (38.247104°N, 122.366210°W) and NE (38.247982°N, 122.361995°W). The vineyard block selected for the study, ES10, totaled 3.63 ha and was planted in 1991. It consisted of a uniform planting of 2,697 vines ha^{-1} of a single cultivar (*Vitis vinifera* L. cv. Pinot noir UC2A) grafted onto the rootstock *V. riparia* x *V. rupestris*, cv. 3309C. The training system was a unilateral cordon trained to 0.8 m with 1.5 m within-row spacing between vines. Rows were 2.4 m apart and ran from east to west with wooden posts supporting the training wires. Vines were vertical shoot-positioned with two pair of shoot-positioning wires at 1.4 m and 2.0 m heights. Irrigation, tillage, and pest and weed management were uniformly applied throughout 2005.

Water status indicators. One hundred and fifty vines were selected in a regular grid pattern of 8.5 m x 24 m. Vines were monitored for two months to track both water-stressed and unstressed vines, defined by periodic measures of Ψ_{PD} and Ψ_{stem} and driven by differences in soil available water and spatial variation in turbulent flux within the vineyard (A. Breazeale and D.R. Smart, 2006, unpublished data). Twenty-five (13 stressed and 12 unstressed) of the 150 vines were selected for more detailed analysis. On 19 Sept 2005, when the canopy was in a nonsenescent state, $\Psi_{PD,}$ $\Psi_{stem,}$ canopy, and leaf reflectance measurements were acquired simultaneously on a subpopulation of leaves. Fresh leaf weights were measured near the mid-afternoon time of maximum water stress. Additional fresh leaf weights and reflectance measurements were collected in the same manner at the canopy level during the subsequent three days.

A leaf pressure chamber (model 3005; Soil Moisture Equipment, Santa Barbara, CA) was used to measure leaf water potential (Ψ_{PD} and Ψ_{stem}), following a proposed method (Turner and Jarvis 1982). All measurements were done on mature leaves located on the midday sunlit (south) side of the vines. Ψ_{PD} was determined on one leaf per vine, beginning at 0400 hr and finishing before sunrise. Periodic measurements of Ψ_{PD} were acquired from a second leaf on the vine, but insignificant leaf-to-leaf variation existed in vine Ψ_{PD}. Midday stem water potential measurements were taken by enclosing a leaf for 20 min in a light-impenetrable plastic bag to arrest transpiration, after which leaf water potential was determined (Ψ_{stem}). Five leaves per vine were measured as somewhat greater leaf-to-leaf variation was encountered within each vine for Ψ_{stem} as compared with Ψ_{PD}. Three leaves analyzed for Ψ_{stem} were collected from the upper canopy (at ~2 m) and two from the lower part of the canopy, ~0.35–0.40 m apart. Leaves in the upper positions were ~3 to 4 weeks younger than leaves in the lower canopy positions, as the youngest leaves had been removed by hedging and no leaves from laterals were used.

Five additional leaves were collected from each vine following the distribution pattern described above. Leaves were weighed immediately to determine fresh weight and then transported to the laboratory in plastic bags on ice and oven dried until reaching a constant dry weight (~48 hr at 55°C). EWT, WCd, and WCt were calculated following equations 1, 2, and 3, respectively, where LA is leaf area (cm^2), Wt is total leaf weight (g), and Wd is oven-dry leaf weight (g) of the same sample. For WCd and WCt, water content as a percent of dry mass (Wd; eq. 2) or water content as a percent of total mass (Wt; eq. 3) were calculated. Specific leaf weight, grams of dry mass per cm^2 of leaf area (SLW), and total specific leaf fresh weight (TSLW) were also calculated.

$$\text{EWT} \left(\frac{g}{cm^2}\right) = \frac{Wt - Wd}{LA} \qquad (1)$$

$$\text{WCd (\%)} = \frac{Wt - Wd}{Wd} * 100 \qquad (2)$$

$$\text{WCt (\%)} = \frac{Wt - Wd}{Wt} * 100 \qquad (3)$$

Water status indicators were analyzed according to the Kolmogorov-Smirnov and Shapiro-Wilk test, which revealed that Ψ_{PD}, Ψ_{stem} - Ψ_{PD}, and SLW were normally distributed (Table 2), whereas Ψ_{stem}, ETW, WCt, WCd, and TSLW were not. We tested the hypothesis that leaf water status depended on the leaf's position (leaf age) within the vine using ANOVA for normally distributed variables and nonparametric tests (U-Mann-Whitney and W-Wilcoxon) for other variables. Unless otherwise stated, the significance test used throughout the manuscript corresponds to a probability of committing a type I error of $p \leq 0.05$.

Spectral reflectance measurements. Reflectance measurements on 125 vine leaves were conducted using an External Integrating Sphere (model 1800-12S; LI-COR, Lincoln, NE) coupled with a FieldSpec Pro ASD spectrometer (Analytical Spectral Devices, Boulder, CO) that detects reflectance in the 350–2500 nm spectral region. Leaf reflectance data were acquired for two different parts of the leaf following standard recommended protocols (LI-COR) and avoiding major leaf veins. The typical sequence of integrating sphere measurements was to first measure a white barium sulfate reference standard (Ir), a leaf sample (Is), and a dark reading (Id). Assuming that the reflectance of the white barium sulfate reference (*R's*) relative to 100% reflectance is 1, then the relative reflectance of a diffuse

sample (Rs, e.g., a leaf) is:

$$Rs = \frac{(Is - Id)R's}{(Ir - Id)} \qquad (4)$$

While barium sulfate does not produce a 100% reflectance standard, the analysis compared leaf reflectance at specific wavelengths sensitive to water stress indicators, so a correction to 100% was not required. Each leaf panel and dark measurement was the average of three scans, which showed little variance. (A schematic view of a similar integrating sphere is shown in Zarco-Tejada et al. 2005a). Reflectance data were taken for the 125 leaves at four different times: immediately after collecting the leaf in the field (t0), 24 hr later under laboratory conditions (t1), after oven drying the samples for 30 min at 45ºC (t2), and after oven drying the samples for 24 hr (t3).

Canopy radiance was measured with the FieldSpec Pro ASD spectrometer. All spectral data were collected from a nadir orientation. The spectrometer was located at 0.70, 0.50, and 0.30 m above the vine canopy. The field-of-view was 25°, covering a circular area of 0.31, 0.22, and 0.13 m in diameter, respectively. Two diffuse reflectance targets (10% and 50%) were used to calculate reflectance. Both calibration panels were composed of gray Spectralon (Labsphere, North Sutton, NH), a National Bureau of Standards material for diffuse reflectance standards with a reflective area of 8 x 8 inches. A dark current correction was collected with each spectral measurement. Each measurement was from an internal average of three spectra. The spectral bands in some VIs were changed from their original definition by slightly decreasing the spectral bandwidths as specified in Table 1.

Defining linear segments between wavelengths that incorporated the feature of interest approximated the continuum used for CRA. Once established, the difference between the measured spectrum and the continuum was calculated by dividing the original reflectance values by the corresponding values of the continuum (Kokaly and Clark 1999). The band depth (D) of each point in the absorption feature was computed by the difference to the continuum,

$$D = 1 - R' \qquad (5)$$

where R' is the measured reflectance value in CRA. The FWHM of the water absorption feature was calculated as the distance (in nm) right to left of the width at half the maximum depth of the absorption feature after the continuum was removed (Figure 1). The end points of the water absorption continua used in this study for the CRA span a range of absorption spectra that start somewhat lower than and end at a longer wavelength (e.g., 2200 nm)
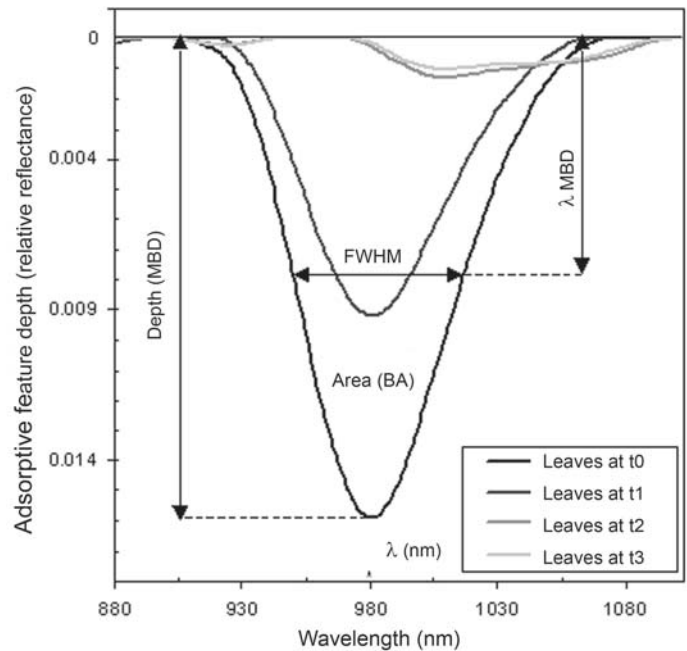

Figure 1 CRA (continuum removed) for 970 nm absorption feature: MBD, BA, IMBD, and FWHM. Plots show average reflectance for 125 leaves at four times: after collection in the field (t0); 24 hr later in the lab (t1); after oven drying samples for 30 min at 45°C (t2); and after complete oven drying of samples (t3).

Table 2 Summary of water status measures for *V. vinifera* cv. Pinot noir clone UC2A growing on *V. riparia* x *V. rupestris* cv 3309C rootstock in the Carneros region, California.

	Ψ_{stem}[a,b] (MPa)	Ψ_{PD}[a,b] (MPa)	$\Psi_{stem} - \Psi_{PD}$[a,b] (MPa)	SLW[a] (kg/m²)	TSLW[c] (kg/m²)	EWT[c] (kg/m²)	WCd[c] (%)	WCt[c] (%)
Average	-1.04	-0.34	-0.71	0.074	0.127	0.076	106.714	42.902
Median	-1.00	-0.28	-0.69	0.077	0.105	0.082	112.977	53.047
SD	0.25	0.16	0.18	0.019	0.062	0.054	77.909	24.435
Minimum	-1.50	-0.66	-1.13	0.038	0.038	9.38E-04	1.042[d]	1.031[d]
Maximum	-0.50	-0.10	-0.16	0.108	0.283	0.186	331.356	76.817
CV	-0.24	-0.45	-0.26	0.252	0.486	0.718	0.730	0.570
n	94	25	94	125[e]	483[e]	340[e]	340[e]	340[e]

[a]Normal distribution fitting by Kolmogorov-Smirnov test.
[b]Normal distribution fitting by Shapiro-Wilk test.
[c]Non-normal distribution fitting.
[d]t3 leaves contained residual water or minor respiratory C loss occurred.
[e]Outliers were discarded.

than the actual feature (Table 3). Wavelength intervals used varied depending on whether the analysis was done at the leaf or canopy levels. Spectral signatures at the canopy level exhibited atmospheric water vapor absorption in wavelengths between 1260–1400 nm and 1800–1950 nm.

Finally, we calculated REIP as the maximum of the first derivative of the spectral reflectance between 670 nm and 780 nm at the canopy level (Broge and Leblanc 2001) to test it as an indicator of water stress of grapevines. For both the leaf and the canopy levels, MBD and λMBD, BA, and FWHM were calculated using IDL visualization software scripts (Research Systems, Boulder, CO) following definitions explained above.

Results

Water status. No vertical location (age related) differences were found for any of the measures of Ψ or EWT, but important differences were found for SLW, TSLW, WCd, and WCt, depending on the position of the leaf (Table 4). Younger leaves located at the top of the vine, in positions 1, 3, and 5, were heavier than older leaves located on shoots at the bottom of the canopy, in positions 2 and 4. Consequently, leaves near the top of the canopy had more dry matter and water than leaves situated in the lower canopy levels, therefore higher SLW and TSLW, and thus water content estimated using WCd or WCt was greater at the top than at the bottom of the vine canopy.

Individual leaf reflectance varied significantly with drying time (Figure 2). Changes in reflectance were similar for leaves of stressed vines (Ψ_{stem} - Ψ_{PD} < -0.85 MPa) and nonstressed vines (Ψ_{stem} - Ψ_{PD} > -0.45 MPa). Differences in reflectance between leaves of stressed and nonstressed vines (Figure 2) were more easily detected in the CRA for the water absorption feature at 970 nm (Figure 1). Averages and standard deviations of canopy reflectance measured at 0.3, 0.5, and 0.7 m above vine height were used to identify the wavelength position of features in the CRA spectra at canopy level (Table 3).

Leaf water status. Pearson correlation coefficients (R) were calculated for apparent correlations between param-

eters that underwent CRA and water status indicators at the leaf level (Table 5). In general, MBD and BA within the water absorption features of 970, 1160, 1460, and 2020 nm were highly correlated with all leaf water content indicators (EWT, WCt, and WCd). Considering EWT, R increased to 0.96 using MBD at the 970 nm absorption feature. Similar values were realized with MBD and BA at 1160 nm (R = 0.95), and BA only at 970 and 1460 nm (R = 0.94). WCd and WCt were also strongly correlated but with generally much lower correlation coefficients than EWT, with the exception of WCt at 1460 and 2020 nm, where R increased to 0.94 for MBD and BA. λMBD and FWHM were generally only weakly correlated with leaf water content; however, for λMBD at 1740 nm R = 0.83.

Several VIs at the leaf level produced excellent correlations with water content indicators with R values >0.90. Correlations using EWT were generally better than those using either WCd or WCt. The best results were obtained using Simple Ratio (SR2) (R = 0.96), Moisture Stress (MSI1) (R = 0.95), Simple Ratio Water 2 (SRWI2) (R = -0.94), Normalized Difference Water (NDWI2) (R = 0.93), Water (WI) (R = 0.92), and Shortwave Infrared Water Stress (SIWSI) (R = 0.91) indexes (Table 5). The same VIs provided the best correlations to estimate leaf water content in terms of WCd values, but the R values achieved were somewhat lower than for EWT. The best results for WCd were observed for SR2 (R = 0.87), MSI1 and WI (R = 0.86), and SRWI2 (R = -0.86). Similar results were also obtained for WCt against the same VIs. The Cellulose Absorption Index (CAI), which has a strong absorption feature (2000–2200 nm), overlapped with the 2020 feature reported in this investigation and was strongly negatively

Table 3 Location of reflectance features used in the continuum removal analysis at the leaf level (LL) and canopy level (CL) (values in nm).

Designation of abs feature		Short wavelength end		Center		Long wavelength end	
LL	CL	LL	CL	LL	CL	LL	CL
700	700	550	550	715	715	880	880
970	970	880	880	975	975	1070	1070
1160	1260	1070	1070	1165	1165	1260	1260
1460	—	1260	—	1460	—	1660	—
—	1600	—	1400	—	1600	—	1800
1740	—	1660	—	1742.5	—	1825	—
2020	—	1825	—	2025	—	2225	—
—	2200	—	1950	—	2187.5	—	2425

Table 4 Mean separation for specific leaf weight, total specific leaf fresh weight, water content as a percent of dry mass, and water content as a percent of total fresh mass for different positions (leaf ages) in the canopy. Positions 1, 3, and 5 were in the upper part of the canopy (2 m); positions 2 and 4 were in the lower part of the canopy (1.5–1.6 m, or just above the fruiting zone).

Positions	SLW (kg/m²)	TSLW (kg/m²)	WCd (%)	WCt (%)
1-2	**a	**	*	*
1-3	ns	ns	ns	ns
1-4	**	**	*	*
1-5	ns	ns	ns	ns
2-3	**	**	*	*
2-4	ns	ns	ns	ns
2-5	**	**	*	*
3-4	**	**	*	*
3-5	ns	ns	ns	ns
4-5	**	**	**	**
Test[b]	a, b	c, d	a, b	a, b

[a]*, **, and ns indicate significance at $p < 0.05$, 0.01, and not significant, respectively.
[b]Statistical tests: (a) U of Mann-Whitney; (b) W of Wilcoxon; (c) HSD of Tukey; (d) GH of Games-Howell.
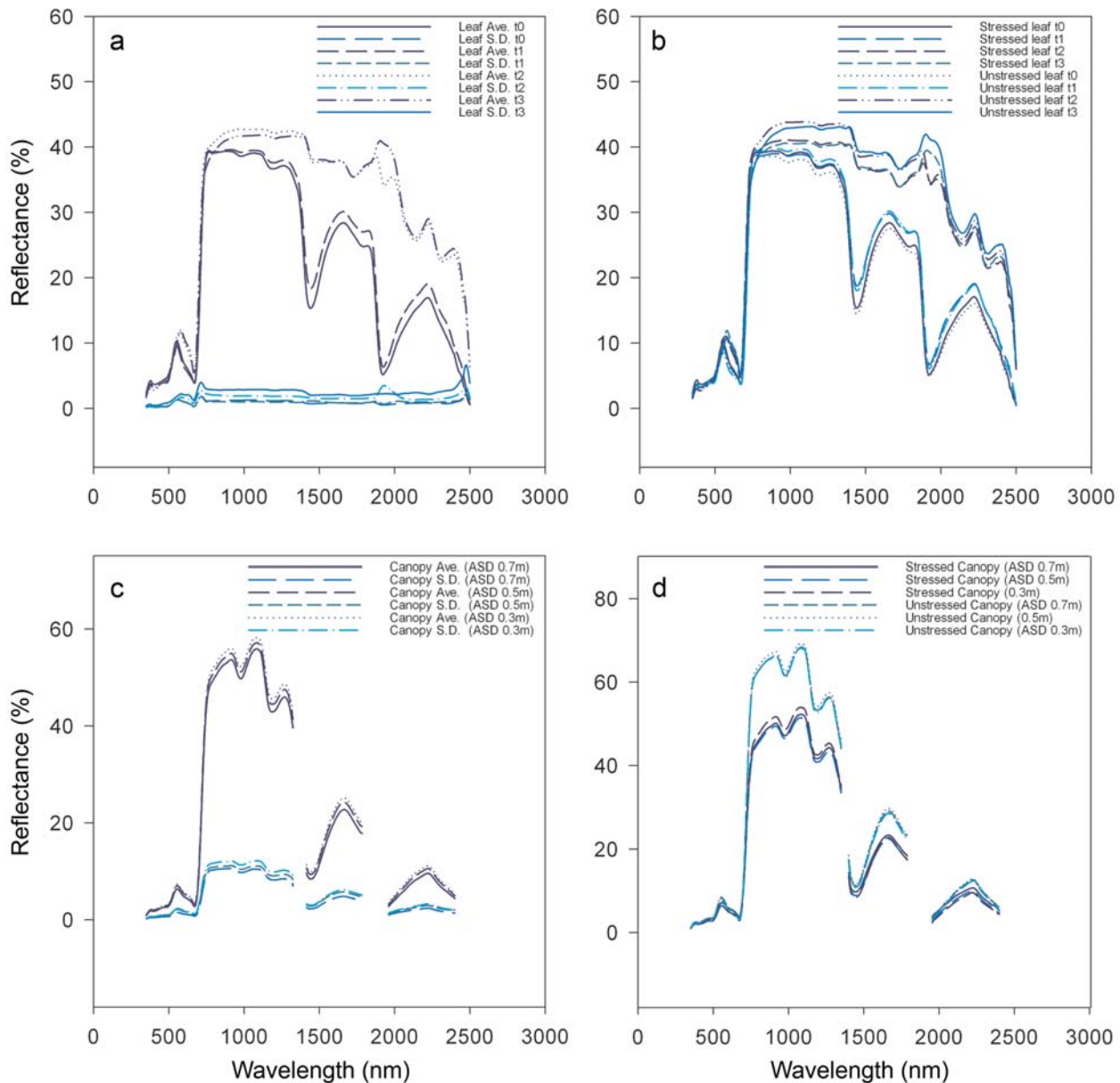
Figure 2 Spectral signatures of 125 leaves and leaf canopies. (**a**) Spectra from 125 leaves collected at four times with an integrating sphere; after collecting the leaves in the field (t0); 24 hr later in the lab (t1); after oven drying samples for 30 min at 45°C (t2); after complete oven drying of samples for 25 hr at 55°C (t3). Average and standard deviation reflectance values noted in the plots. (**b**) Average reflectance values for leaves of four stressed vines (Ψ_{stem} - Ψ_{PD} less than -0.85 MPa) and four nonstressed vines (Ψ_{stem} -Ψ_{PD} greater than -0.45 MPa). (**c**) Average and standard deviation of canopy reflectance values of 25 vines measured with an analytical spectral device at 0.3, 0.5, and 0.7 m above the canopy. (**d**) Average reflectance values for four stressed vines (Ψ_{stem} - Ψ_{PD} less than -0.85 MPa) and four nonstressed vines (Ψ_{stem} - Ψ_{PD} greater than -0.47 MPa), both at the three acquisition heights (0.3, 0.5, and 0.7 m). Wavelengths with high atmospherics absorbance (1350 and 1850 nm) were not included in plot.

correlated with WCt (R = -0.93), even though these were not dry leaves. The best result was observed for SR2 (R = 0.94) (Table 5). Vine Ψ measurements were poorly correlated with both CRA parameters and VIs at the leaf level and results are not shown.

    Canopy water status. Results obtained at the canopy level based on the Pearson correlation coefficients between REIPv, MBD, BA (CRAs), and other VIs with EWT and vine water potential (Ψ_{stem} and Ψ_{stem} - Ψ_{PD}) are shown in Table 6. Correlations between the CRA and water status indicators were lower at canopy level than leaf level for all three above-canopy ASD positions. The best results were

those obtained using the ASD at the 0.7 m position; results for 0.5 and 0.3 m positions are therefore not shown. At the finest scale, leaf gaps, shading, and differences in leaf angle increase measurement heterogeneity, which is reduced at the larger scale by spectral averaging. In most cases Ψ measurements at the canopy scale yielded higher R values than any of the leaf water content measures. In general, results at 0.3 and 0.5 m above the canopy also exhibited this tendency but R values were generally much lower. R values for REIP, λMBD, FWHM and Ψ_{PD}, WCd, or WCt that were below 0.55 are not given for the ASD at 0.7 m distance.

Table 5 Pearson correlation coefficients calculated for relationships of equivalent water thickness, water content as percent of dry mass, and water content as percent of total fresh mass measured at the leaf level, with continuum removal analyses performed at six waveband intervals (Table 3) and various proposed vegetation indexes. Table includes R values <-0.70 or >0.70 (significant correlation at $p < 0.01$ confidence level).

	EWT(kg/m²)[a]	WCd (%)[b]	WCt (%)[a]
CRA/VI			
BA$_{700\ nm}$	—	—	0.78
MBD$_{970\ nm}$	0.96	0.83	0.84
λ MBD$_{970\ nm}$	-0.68	-0.68	-0.75
BA$_{970\ nm}$	0.94	0.82	0.82
MBD$_{1160\ nm}$	0.95	0.81	0.89
λ MBD$_{1160\ nm}$	0.79	0.78	0.91
BA$_{1160\ nm}$	0.95	0.80	0.89
MBD$_{1460\ nm}$	0.92	0.85	0.94
λ MBD$_{1460\ nm}$	—	—	-0.71
BA$_{1460\ nm}$	0.94	0.85	0.93
λ MBD$_{1740\ nm}$	0.83	0.85	0.94
MBD$_{2020\ nm}$	0.85	0.84	0.94
λ MBD$_{2020\ nm}$	-0.75	-0.75	-0.86
BA$_{2020\ nm}$	0.89	0.84	0.94
RGI	-0.80	-0.80	-0.90
RGI1	-0.76	-0.76	-0.87
BRI	0.79	0.77	0.85
BRI1	0.77	0.72	0.83
BRI2	0.79	0.77	0.86
SR1	—	—	-0.77
SR2	0.96	0.87	0.94
RBI	-0.73	-0.71	-0.80
MSI	-0.90	-0.77	-0.85
MSI1	0.95	0.86	0.92
mNDVI	—	—	0.73
VI			
PRI3	—	-0.76	-0.82
NPCI	-0.74	-0.75	-0.84
SRPI	0.76	0.77	0.85
SIPI	—	—	-0.74
SIPI1	—	—	-0.72
NDNI	0.87	0.81	0.87
CAI	-0.80	-0.83	-0.93
NDWI	0.89	0.82	0.88
NDWI1	0.88	0.82	0.88
NDWI2	0.93	0.84	0.92
WBI	-0.92	-0.86	-0.90
WI	0.92	0.86	0.90
fWBI	0.91	0.85	0.89
SRWI	0.89	0.82	0.88
SRWI1	0.91	0.84	0.89
SRWI2	-0.94	-0.86	-0.93
SRWI3	0.91	0.84	0.89
Crt1	-0.72	-0.71	-0.81
Crt2	—	—	-0.77
Crt3	-0.72	-0.71	-0.80
Lic1	0.79	0.77	0.86
Vog	—	—	0.71
GM2	—	—	0.70
NDII	0.91	0.76	0.84
SIWSI	0.91	0.77	0.85

[a]n = 340. [b]n = 350.

Table 6 Pearson correlation coefficients calculated for relationships of Ψ_{stem}, Ψ_{stem} - Ψ_{PD}, and equivalent water thickness measured at the canopy level, with continuum removal analyses performed at five waveband intervals (Table 3) and various proposed vegetation indexes. Table includes R values <-0.55 or >0.55.

	Ψ_{stem} (MPa)	Ψ_{stem} - Ψ_{PD} (MPa)	EWT (kg/m²)
CRA/VI			
REIPv	—	—	0.59**
MBD$_{700\ nm}$	0.58**[a]	0.71**	—
BA$_{700\ nm}$	—	0.66**	—
MBD$_{1600\ nm}$	0.63**	0.72**	—
BA$_{1600\ nm}$	0.67**	0.69**	—
GI	0.56*	0.57*	—
RGI	-0.68**	-0.79**	—
RGI1	-0.66**	-0.76**	—
RVI	—	0.59**	—
GRR	0.56*	0.57*	—
NGRR	-0.57**	-0.62**	—
NGRR1	—	0.69**	—
SR	—	0.61**	—
SR1	—	-0.66**	—
SR3	—	-0.69**	—
SR4	—	-0.68**	—
DVI	—	—	0.58**
NDVI	—	0.69**	—
NDVI1	—	0.69**	—
NDVI2	—	0.68**	—
NDVI3	—	0.69**	—
NDVI4	—	0.69**	—
mNDVI	—	0.55*	—
PRI3	—	-0.55*	—
VI			
NPCI	—	-0.62*	—
SRPI	—	0.61**	—
SIPI	-0.59**	-0.74**	—
SIPI1	-0.55*	-0.72**	—
NDNI	—	0.61**	0.55**
NDLI	—	—	0.57**
NDWI	0.57*	0.58**	—
NDWI1	0.57**	0.58**	—
WBI	—	-0.56*	—
WI	—	0.56*	—
fWBI	0.55*	0.57*	—
SRWI	0.57*	0.57**	—
MCARI	—	0.62**	—
MTVI1	—	—	0.58**
MTVI2	—	0.63**	—
MTVI3	—	-0.56*	-0.60**
RDVI	—	—	0.58**
MSR	—	0.64**	—
TVI	—	—	0.59**
TVI1	—	—	0.59**
Crt2	—	-0.66**	—
Lic	0.56*	0.70**	—
GM2	—	0.60**	—
EVI	—	0.57*	0.56**

[a]* and ** indicate significant correlation at $p < 0.05$ and 0.01 confidence levels, respectively; n = 19.

When ASD data were collected at 0.50 m above the canopy, the best Pearson correlation coefficient was for EWT and REIPv (R = 0.61). Generally, R for EWT was better than for WCd and WCt at all ASD positions. The best result using WCd was observed for λMBD at 700 nm (R = 0.52), and for WCt the best results were obtained for MBD or BA at 2200 nm (R = -0.55) and ASD at 0.7 m over the canopy, (R = -0.56).

The estimation of vine Ψ using CRA showed that Ψ_{PD} had a low correlation with all spectral measures while Ψ_{stem} yielded improved correlations. The Ψ_{stem} - Ψ_{PD} difference yielded the best relationships. Correlations with ASD data obtained at 0.7 m above the canopy again were higher than those at shorter distances. The absorption features at 700 and 1600 nm produced R values of 0.71 and 0.72 for MBD and 0.66 and 0.69 for BA, respectively (Table 6).

Correlations of the water potential difference of Ψ_{stem} - Ψ_{PD} with VIs provided better results than with other water potential indicators. Red/Green indexes, RGI and RGI2, had R values of -0.79 and -0.76, respectively, whereas the SIPI had an R value of -0.74. Correlations for EWT using MTVI3 also produced better results than other VIs such as TVI or MCARI1, but the absolute value of R was still less than 0.70. The best correlation for WCd was observed for RGI (R = -0.50). For WCt, the best performing VIs were MTVI3 (R = -0.51) and TVI (R = 0.51).

Leaf and canopy water status correlations. Linear correlations were calculated to estimate water status using CRA at leaf level (Figure 3). MBD gave good estimates of WCd, WCt, and EWT. The best linear correlation for EWT was achieved using MBD at the 970 nm absorption feature, but similar values were obtained for BA at 1160 nm (Figure 3a, b). WCd was fairly well correlated with MBD and BA at 1460 nm, and estimations of WCd varied by more than half of a standard deviation (Figure 3c, d). Data were distributed at the extremes on the regression line, and this bimodal distribution strongly affected the results for BA and MBD. WCt was better estimated from CRA than was WCd. λMBD at 1740 nm was strongly correlated with WCt (Figure 3e). Bipolar distribu-
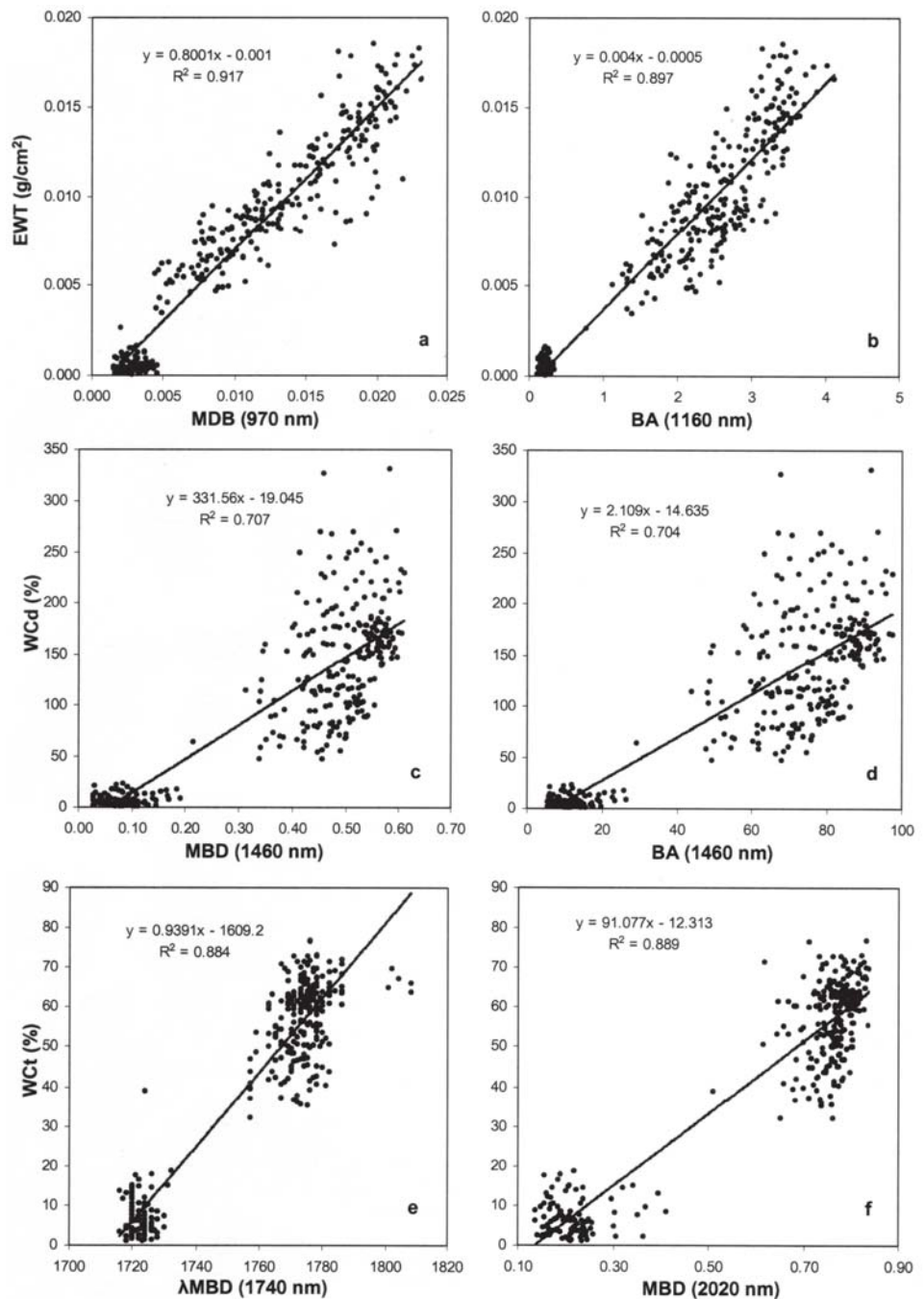

Figure 3 Linear correlations to estimate water content using CRA at the leaf level: EWT estimation by (**a**) MBD at 970 nm (RMSE = 1.57 mg/cm^2) and (**b**) BA at 1160 nm (RMSE = 1.74 mg/cm^2). WCd estimation by (**c**) MBD at 1460 nm (RMSE = 42.26%) and (**d**) BA at 1460 nm (RMSE = 42.44%). WCt estimation by (**e**) lMBD at 1740 nm (RMSE = 8.33%) and (**f**) MBD at 2020 nm (RMSE = 8.15%).

tion of the data was most obvious using the MBD at 2020 nm (Figure 3f). A number of VIs were useful in estimating EWT and produced R^2 values >0.80: RGI, SR2, MSI, MSI1, Normalized Difference Nitrogen (NDNI), CAI, Normalized Difference Water (NDWI), NDWI1, NDWI2, Water Band (WBI), WI, Floating Positive Water Band (fWBI), SRWI, SRWI1, SRWI2, SRWI3, Normalized Difference Infrared (NDII), and SIWSI (see Table 1 for further information). Linear correlations using VIs were of similar accuracy to estimates from CRA; the best results were obtained with
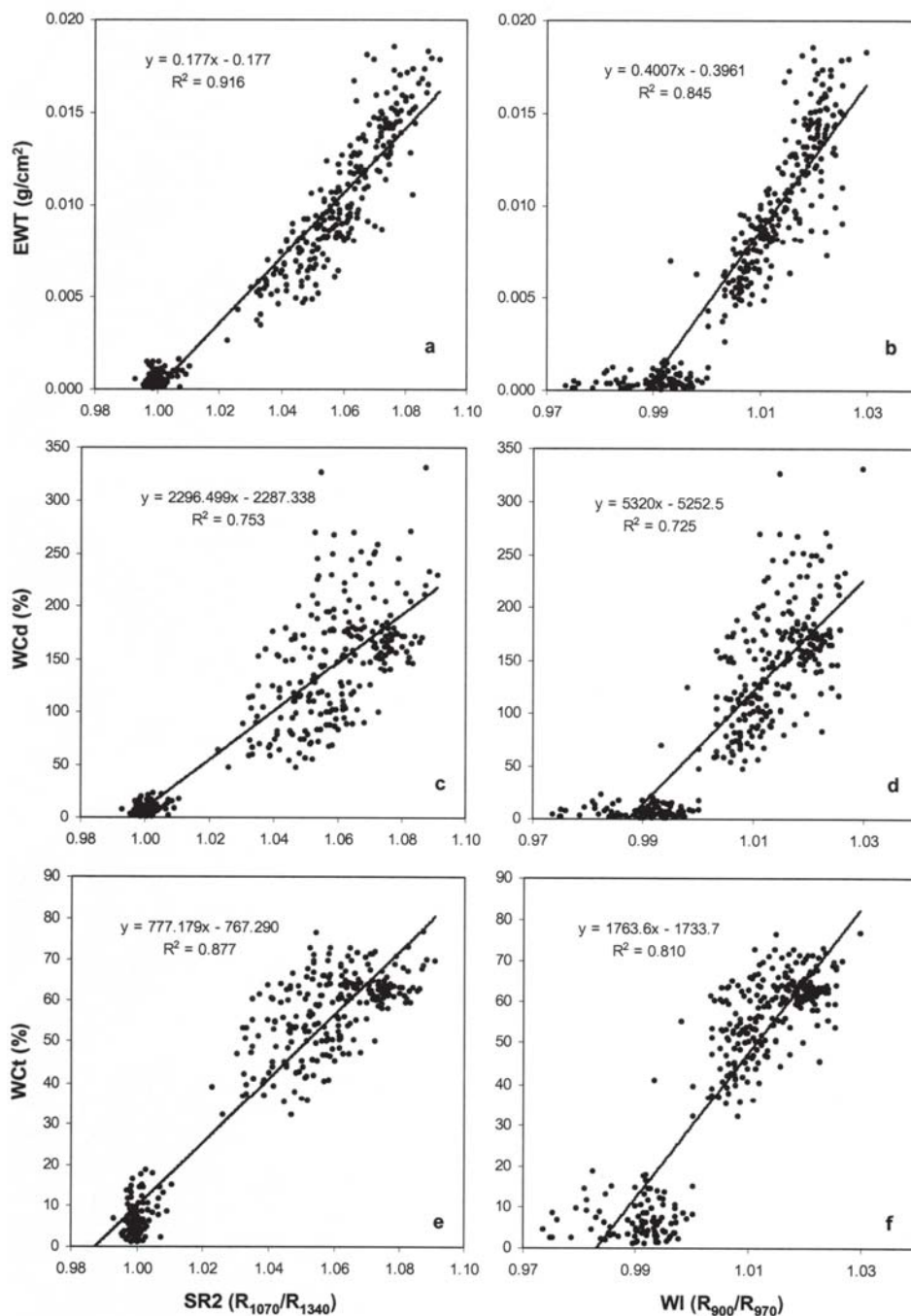
Figure 4 Linear correlations to estimate water content using vegetation indexes (VI) evaluated at the leaf level: EWT estimation by (**a**) SR2 (RMSE = 1.58 mg/cm^2) and (**b**) WI (RMSE = 2.14 mg/cm^2). WCd estimation by (**c**) SR2 (RMSE = 38.77%) and (**d**) WI (RMSE = 40.93%). WCt estimation by (**e**) SR2 (RMSE = 8.56%) and (**f**) WI (RMSE = 10.67%).

variation (Figure 5a). The linear regression of vine Ψ and BA explained less of the variation (Figure 5b). Ψ_{stem} and $\Psi_{stem} - \Psi_{PD}$ were more highly correlated to RGI and SIPI than they were to results obtained using CRA (Figure 5c, d).

Discussion

Variation in leaf and canopy reflectance followed the expected responses to water content at both the leaf (Figure 2a, b) and canopy (Figure 2c, d) levels. In other words, reflectance increased with leaf drying for both stressed and nonstressed leaves. Strong light absorption by photosynthetic pigments was detected for green leaves in the visible spectral range (VIS 400–700 nm), and this absorption increased with leaf hydration status (Figure 2a). The physiological dependence of leaf pigments on water is responsible for high correlations observed between water status and various pigment sensitive VIs, even though water does not absorb energy in this wavelength region. The NIR plateau (700–1300 nm) is characterized by light absorption by dry matter, while reflectance in this region is controlled by scattering processes that are driven by the internal structure of palisade parenchyma and spongy mesophyll of the leaves (Jacquemoud and Ustin 2001). In the SWIR, absorption is strongly influenced by water in moist leaves, which decreases as the leaves dry (Figure 2a,b) (Jacquemoud and Ustin 2001). This pattern extends to the canopy level, as shown by the measurements taken at three heights (Figure 2c). Water absorption features are likely stronger at the canopy than at the leaf level because of higher overall canopy water content as leaf area density increases. As a result, differences between water stressed and nonstressed vines are more clearly observed as canopy reflectance (Figure 2d).

The examined water absorption features provided strong evidence that it would be possible to detect water stress as a function of desiccation through water content indicators such as EWT, WCd, and WCt. These water content indicators were highly significantly correlated ($p = 0.01$) with CRA parameters at the leaf level (Table 5). The
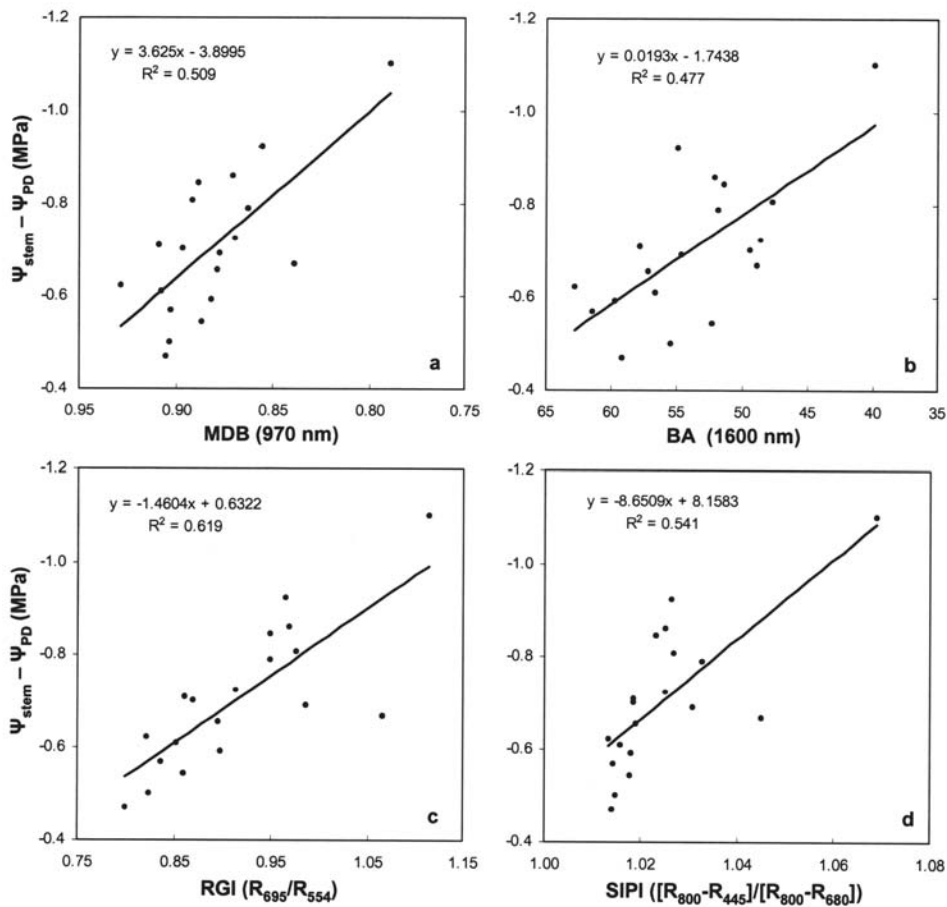
SR2 and WI, and EWT was better estimated than either WCt or WCd (Figure 4).

The analysis at the canopy level suggested that vine Ψ could be estimated using both CRA and VIs at the local level (e.g., individual leaves or from measurements at 0.7 m above the canopy). Several linear regressions with high R^2 values were proposed for estimation of vine predawn versus midday Ψ difference ($\Psi_{stem} - \Psi_{PD}$) (Figure 5). The equation used to estimate is shown in Figure 5a. The linear regression of vine Ψ by MBD explained 51% of the

Figure 5 Estimation of the difference between predawn and midday stem water potential (Ψ_{stem} - Ψ_{PD}) measured at the canopy level by (**a**) MBD at 970 nm (RMSE = 0.113 MPa), (**b**) BA at 1600 nm (RMSE = 0.116 MPa), (**c**) RGI (RMSE = 0.099 MPa), and (**d**) SIPI (RMSE = 0.109 MPa).

For the 79 VIs that were evaluated (Table 1), most if not all showed good correlations with water content (WCt, g water/g fresh weight) when measured at the leaf level using the integrating sphere (Table 5). Thus, the influence of water content in grape leaves clearly had a sufficiently strong influence on leaf reflectance that remote detection (from field, aircraft or satellite measurements) of leaf water status (on a relative basis) may be achievable. Nonetheless, for 69 of the VIs, significant correlations were not found for the EWT (Danson et al. 1992, Ceccato et al. 2001). For midday stem water potential (Ψ_{stem}, MPa), a generally reliable indicator of vine water stress under field conditions (Williams and Trout 2005), correlations with VIs were somewhat better, but these were not always the same VIs that were significantly correlated with EWT (Table 6). The difference between Ψ_{stem} - Ψ_{PD} was the most reliable indicator of water status and was significantly correlated with over 70 of the VIs evaluated (Table 6). Thus, it appeared that at the canopy level, relative stress, at least on a diurnal basis, could be remotely detected even though the correlations with leaf water content (EWT) were somewhat weak. Again, this may be due to the fact that water content throughout the canopy was not uniform (Table 2) while Ψ_{stem} showed less variability for leaves in full sun.

The Simple Ratio Vegetation index 2 (SR2, this study), which uses the water absorption features at 1070 and 1340 nm (R_{1070}/R_{1340}), was the most effective VI to detect EWT at the leaf level. Therefore, we propose this new index as a possible means to remotely estimate water status in vineyards. The Water index (WI) focuses on the water absorption peak near 970 nm (R_{900}/R_{970}), and this ratio increased with water stress at the leaf level indicating lower leaf water content (Peñuelas et al. 1997a). Nonetheless, WI was not nearly as robust an estimator of water status as were other VIs at the canopy level (Table 6). Similar results were reported by other researchers using IR water absorption wavelengths (Peñuelas et al. 1993, Jones et al. 2004).

Water potential, principally Ψ_{stem} - Ψ_{PD}, was related to spectral patterns at the canopy level. It must be noted that the Ψ_{stem} - Ψ_{PD} difference may not always represent vine water stress. Substantial xylem refilling at night coupled with high evapotranspiration demand at midday might produce a large Ψ_{stem} - Ψ_{PD} difference, which only indicates short duration (midday) stress. Conversely, a low

most useful water absorption features were at 970, 1160, and 1460 nm, and the best results were achieved using MBD and BA, which is in general agreement with previous studies of other higher plant species (Jones et al. 2004). The indicators used to estimate leaf water status, EWT, WCd, or WCt in this investigation each have different correspondence with stress. Thus, these indicators of water status are mostly *relative* indicators of hydration status with respect to time.

Strong correlations were found for both WCd and WCt, but they were somewhat better for EWT (Figures 3 and 4). Again, this result was likely influenced by the fact that WCd and WCt strongly depended on the position (age) of the sampled leaves on the vine. In addition, because EWT is weighted to leaf area, it may better match the reflective surface as a function of water status. The best correlation to estimate EWT at the leaf level was observed for MBD at the 970 nm water absorption feature (R^2 = 0.917; Figure 3a). The fact that EWT was not affected by canopy position, and thus leaf age, suggests this parameter may be more appropriate for use in predicting vine water status. This result may indicate that EWT will be less dependent on the general orientation of the canopy by the trellis system.

Ψ_{PD}, even when coupled with high midday evaporation demand, can produce a small Ψ_{stem} - Ψ_{PD} difference, yet in this case, vines would experience water stress through growth reduction (Smart et al. 2006). Nonetheless, in the vineyard studied for this investigation, larger Ψ_{stem} - Ψ_{PD} differences corresponded with a high degree of water stress and premature leaf senescence. This work supports results obtained in similar studies for other plant taxa: PRI, NDVI, and WBI were correlated with water potential in sunflower leaves, with Pearson correlation coefficients of -0.74, -0.44, and 0.33 respectively (Peñuelas et al. 1994). Mogensen et al. (1996) related relative reflectance index and leaf water potential in oilseed rape for different soil textures. And in drought-stressed *Pinus edulis*, water content correlated strongly with NDWI ($R^2 = 0.93$) and for a continuum calculated at 980 nm ($R^2 = 0.91$) (Stimson et al. 2005). Water potential in that study was weakly correlated with a 980 nm continuum ($R^2 = 0.37$).

In the current investigation, RGI was the vegetation index that achieved the best result for estimating water potential at the canopy level, apparently because of heightened sensitivity in the visible region to physiological changes in vine canopies. However, because water absorbs energy less efficiently than chlorophyll, indexes based on the water absorption bands allow deeper penetration into thick canopies than indexes based on chlorophyll absorption features alone (Sims and Gamon 2003). Estimates of water content at the leaf level were better than those at the canopy level because of large variation in reflectance among canopy leaves at similar levels of water stress and are further subject to changes associated with canopy geometry (Table 4) (Serrano et al. 2000).

Conclusions

We identified several vegetation indexes that may be useful for remote sensing of grapevine water status and water stress. Despite the observed heterogeneity of water content in field canopies, variation in reflectance at the canopy level may be due to canopy shape, sun, or sensor perspective. Nonetheless, consistent changes in reflectance are associated with declining water potential and changes in leaf turgor, an association supported in the present study. This further supports that field spectrometer measurements may have potential applications in commercial vineyards to detect water status in vines, particularly if the analytical spectral device is tractor mounted, for example, and installed at the positions found suitable in this investigation (0.7 m). EWT provided the best leaf water content indicator related to water absorption features measured using an integrating sphere. EWT may be estimated by MBD at 970 nm or by BA at 1160 nm, and using VIs such as the SR or WI families of indicators. While less accurate than leaf level reflectance, canopy reflectance was more useful in estimating Ψ than any other indicator as a function of leaf area. Ψ was correlated with reflectance at the canopy level and it was possible to estimate Ψ_{stem} - Ψ_{PD} by linear correlation with

RGI (R_{695}/R_{554}). The employment of such techniques may allow vine growers a more efficient method to manage irrigation scheduling in large-scale vineyards or when numerous large vineyard blocks are managed from tractor-mounted, top-of-canopy systems, or from airborne and satellite imaging.

Literature Cited

Bahrun, A., V.O. Mogensen, and C.R. Jensen. 2003. Water stress detection in field-grown maize by using spectral vegetation index. Comm. Soil Sci. Plant Anal. 34:65-79.

Barnes, J.D. 1992. A reappraisal of the use of DMSO for the extraction and determination of chlorophylls a and b in lichens and higher plants. Environ. Exp. Bot. 2:85-100.

Bowman, W.D. 1989. The relationship between leaf water status, gas exchange, and spectral reflectance in cotton leaves. Remote Sens. Environ. 30:249-255.

Broge, N.H., and E. Leblanc. 2001. Comparing prediction power and stability of broadband and hyperspectral vegetation indices for estimation of green leaf area index and canopy chlorophyll density. Remote Sens. Environ. 76:156-172.

Broge, N.H., and J.V. Mortensen. 2002. Deriving green crop area index and canopy chlorophyll density of winter wheat from spectral reflectance data. Remote Sens. Environ. 81:45-57.

Carter, G.A. 1994. Ratios of leaf reflectances in narrow wavebands as indicators of plant stress. Int. J. Remote Sens. 15:697-704.

Carter, G.A., T.R. Dell, and W.G. Cibula. 1996. Spectral reflectance characteristics and digital imagery of a pine needle blight in the southeastern United States. Can. J. For. Res. 26:402-407.

Ceccato, P., S. Flasse, S. Tarantola, S. Jacquemoud, and J.M. Gregoire. 2001. Detecting vegetation leaf water content using reflectance in the optical domain. Remote Sens. Environ. 77:22-33.

Chen, J. 1996. Evaluation of vegetation indices and modified simple ratio for boreal applications. Can. J. Remote Sens. 22:229-242.

Chuvieco, E., D. Riaño, I. Aguado, and D. Cocero. 2002. Estimation of fuel moisture content from multitemporal análisis of Landsat Thematic Mapper reflectance data: Applications in fire danger assessment. Int. J. Remote Sens. 23:2145-2162.

Cifre, J., J. Bota, J.M. Escalona, H. Medrano, and J. Flexas. 2005. Physiological tools for irrigation scheduling in grapevine (*Vitis vinifera* L.). An open gate to improve water-use efficiency? Agric. Ecosyst. Environ. 106:159-170.

Clark, R.N. 1999. Spectroscopy of rocks and minerals, and principles of spectroscopy. *In* Manual of Remote Sensing. Vol. 3. Remote Sensing for the Earth Sciences. A.N. Rencz (Ed.), pp. 3-58. Wiley & Sons, New York.

Curran, P.J., J.L. Dungan, and D.L. Peterson. 2001. Estimating the foliar biochemical concentration of leaves with reflectance spectrometry: Testing Kokaly and Clark methodologies. Remote Sens. Environ. 76:349-359.

Danson, F.M., M.D. Steven, T.J. Malthus, and J.A. Clark. 1992. Highspectral resolution data for determining leaf water content. Int. J. Remote Sens. 13:461-470.

Daughtry, C.S.T., C.L. Walthall, M.S. Kim, E. Brown de Colstoun, and J.E. McMurtrey III. 2000. Estimating corn leaf chlorophyll concentration from leaf and canopy reflectance. Remote Sens. Environ. 74:229-239.

Dobrowski, S.Z., J.C. Pushnik, P.J. Zarco-Tejada, and S.L.Ustin. 2005. Simple reflectance indices track heat and water stress-induced changes in steady-state chlorophyll fluorescence at the canopy scale. Remote Sens. Environ. 97:403-414.

Donovan, L., D.J. Grise, J.B. West, R.A. Rappert, N.N. Alder, and J.H. Richards. 1999. Predawn disequilibrium between plant and soil water potentials in two cold-desert shrubs. Oecologia 120:209-217.

Fensholt, R., and I. Sandholt. 2003. Derivation of a shortwave infrared water stress index from MODIS near- and shortwave infrared data in a semiarid environment. Remote Sens. Environ. 87:111-121.

Fischer, C., A. Brunn, C. Dittmann, and P. Vosen. 2003. Detection of plant reflectance anomalies in mining areas using imaging spectroscopy. In Proceedings for the Third EARSeL Workshop on Imaging Spectroscopy. M. Habermeyer et al. (Eds.), pp. 305-312. LDR, Herrsching, Germany.

Flexas, J., J. Briantais, Z.G. Cerovic, H. Medrano, and I. Moya. 2000. Steady state and maximum chlorophyll fluorescence responses to water stress in grapevine leaves: A new remote sensing system. Remote Sens. Environ. 73:283-297.

Fuentes, D.A., J.A. Gamon, H.L. Qiu, D.A. Sims, and D.A. Roberts. 2001. Mapping Canadian boreal forest vegetation using pigment and water absorption features derived from the AVIRIS sensor. J. Geophys. Res. 106:33565-33577.

Gamon, J.A., and J.S. Surfus. 1999. Assessing leaf pigment content and activity with a reflectometer. New Phytol. 143:105-117.

Gamon, J.A., J. Peñuelas, and C.B. Field. 1992. A narrow-waveband spectral index that tracks diurnal changes in photosynthetic efficiency. Remote Sens. Environ. 41:35-44.

Gao, B.C. 1996. NDWI—A normalized difference water index for remote sensing of vegetation liquid water from space. Remote Sens. Environ. 58:257-266.

Gitelson, A.A., and M.N. Merzlyak. 1997. Remote estimation of chlorophyll content in higher plant leaves. Int. J. Remote Sens. 18:2691-2697.

Gitelson, A., Y. Kaufman, and M. Merzlyak. 1996. Use of a green channel in remote sensing of global vegetation from EOS-MODIS. Remote Sens. Environ. 58:289-298.

Haboudane, D., J.R. Miller, N. Tremblay, P.J. Zarco-Tejada, and L. Dextraze. 2002. Integration of hyperspectral vegetation indices for prediction of crop chlorophyll content for application to precision agriculture. Remote Sens. Environ. 81:416-426.

Haboudane, D., J.R. Miller, E. Pattey, P.J. Zarco-Tejada, and I. Strachan. 2004. Hyperspectral vegetation indices and novel algorithms for predicting green LAI of crop canopies: Modeling and validation in the context of precision agriculture. Remote Sens. Environ. 90:337-352.

Hardisky, M.A., V. Klemas, and R.M. Smart. 1983. The influence of soil salinity, growth form, and leaf moisture on spectral radiance of Spartina alterniflora canopies. Photogram. Eng. Remote Sens. 49:77-83.

Huang, Z., B.J. Turner, S.J. Dury, I.R. Wallis, and W.J. Foley. 2004. Estimating foliage nitrogen concentration from HYMAP data using continuum removal analysis. Remote Sens. Environ. 93:18-29.

Huete, A., K. Didan, T. Miura, E.P. Rodríguez, X. Gao, and L.G. Ferreira. 2002. Overview of the radiometric and biophysical performance of the MODIS vegetation indices. Remote Sens. Environ. 83:195-213.

Hunt, E.R., and B.N. Rock. 1989. Detection of changes in leaf water content using near and middle-infrared reflectances. Remote Sens. Environ. 30:43-54.

Hunt, E.R., B.N. Rock, and P.S. Nobel. 1987. Measurement of leaf relative water content by infrared reflectance. Remote Sens. Environ. 22:429-435.

Jacquemoud, S., and S.L. Ustin. 2001. Leaf optical properties: A state of the art. In Proceedings for the Eighth International Symposium Physical Measurements and Signatures in Remote Sensing, pp. 223-232. CNES, Aussois, France.

Jones, C.L., P.R.Weckler, N.O. Maness, M.L. Stone, and R. Jayasekara. 2004. Estimating water stress in plants using hyperspectral sensing. In Proceedings for the ASAE/CSAE Annual International Meeting, 2004. pp. 2-11. Paper 043065. Montreal.

Jordan, C.F. 1969. Derivation of leaf area index from quality of light on the forest floor. Ecology 50:663-666.

Kennedy, J.A., M.A. Matthews, and A.L. Waterhouse. 2002. Effect of maturity and vine water status on grape skin and wine flavonoids. Am. J. Enol. Vitic. 53:268-274.

Kim, M.S., C.S.T. Daughtry, E.W. Chappelle, and J.E. McMurtrey. 1994. The use of high spectral resolution bands for estimating absorbed photosynthetically active radiation (APAR). In Proceedings for ISPRS'94, pp. 299-306. Val d'Isere, France.

Kokaly, R.F., and R.N. Clark. 1999. Spectroscopic determination of leaf biochemistry using band-depth analysis of absorption features and stepwise multiple linear regression. Remote Sens. Environ. 67:267-287.

Kokaly, R.F., D.G. Despain, R.N. Clark, and K.E. Livo. 2003. Mapping vegetation in Yellowstone National Park using spectral feature analysis of AVIRIS data. Remote Sens. Environ. 84:437-456.

Lichtenthaler, H.K., M. Lang, M. Sowinska, F. Heisel, and J.A. Mieh. 1996. Detection of vegetation stress via a new high resolution fluorescence imaging system. J. Plant Physiol. 148:599-612.

Li, L., S.L. Ustin, and M. Lay. 2005. Application of AVIRIS data in detection of oil-induced vegetation stress and cover change at Jornada, New Mexico. Remote Sens. Environ. 94:1-16.

Mbow, C. 1999. Proposition of a method for early fires planning using ground and satellite (NDVI/NOAA-AVHRR) data from Niokolo Koba National Park (Southeast Senegal). In Proceedings for the Second International Symposium on Operationalization of Remote Sensing. Poster presentation. ITC, Enschede, The Netherlands.

McCutchan, H., and K.A. Shackel. 1992. Stem-water potential as a sensitive indicator of water stress in prune trees (Prunus domesticus L. cv. French). J. Am. Soc. Hortic. Sci. 117:607-610.

Mogensen, V.O., C.R. Jensen, G. Mortensen, J. Thage, J. Koribidis, and A. Ahmed. 1996. Spectral reflectance index as an indicator of drought and crop growth in field grown oilseed rape (Brassica napus L.). Eur. J. Agron. 5:125-135.

Nagler, P.L., C.S.T. Daughtry, and S.N. Goward. 2000. Plant litter and soil reflectance. Remote Sens. Environ. 71:207-215.

Pearson, R.L., and L.D. Miller. 1972. Remote mapping of standing crop biomass for estimation of the productivity of the shortgrass prairie, Pawnee National Grasslands, Colorado. In Proceedings for the Eighth International Symposium on Remote Sensing of Environment (ERIM International), pp. 1357-1381. Ann Arbor, MI.

Peñuelas, J., I. Filella, C. Biel, L. Serrano, and R. Savé. 1993. The reflectance at the 950–970 nm region as an indicator of plant water status. Int. J. Remote Sens. 14:1887-1905.

Peñuelas, J., J.A. Gamon, A.L. Fredeen, J. Merino, and C.B. Field. 1994. Reflectance indices associated with physiological changes in nitrogen- and water-limited sunflower leaves. Remote Sens. Environ. 48:135-146.

Peñuelas, J., I. Filella, P. Lloret, F. Muñoz, and M. Vilajeliu. 1995a. Reflectance assessment of mite effects on apple trees. Int. J. Remote Sens. 14:2727-2733.

Peñuelas, J., F. Baret, and I. Filella. 1995b. Semi-empirical indices to assess carotenoids/chlorophyll a ratio from leaf spectral reflectance. Photosynthetica 31:221-230.

Peñuelas, J., J. Lluisa, J. Piñol, and I. Filella. 1997a. Photochemical reflectance index and leaf photosynthetic radiation-use-efficiency assessment in Mediterranean trees. Int. J. Remote Sens. 18:2863-2868.

Peñuelas, J., J. Piñol, R. Ogaya, and I. Filella, 1997b. Estimation of plant water concentration by the reflectance water index (R900/R970). Int. J. Remote Sens. 18:2869-2875.

Reujean, J., and F. Breon. 1995. Estimating PAR absorbed by vegetation from bidirectional reflectance measurements. Remote Sens. Environ. 51:375-384.

Ripple, W.J. 1986. Spectral reflectance relationships to leaf water stress. Photogram. Eng. Remote Sens. 52:1669-1675.

Rouse, J.W., R.H. Haas, J.A. Schell, D.W. Deering, and J.C. Harlan. 1974. Monitoring the vernal advancement of retrogradation of natural vegetation. Type III, final report, pp. 1-371. NASA/GSFC, Greenbelt, MD.

Serrano, L., S.L. Ustin, D.A. Roberts, J.A. Gamon, and J. Peñuelas. 2000. Deriving water content of chaparral vegetation from AVIRIS data. Remote Sens. Environ. 74:570-581.

Serrano, L., J. Peñuelas, and S.L. Ustin. 2002. Remote sensing of nitrogen and lignin in Mediterranean vegetation from AVIRIS data: Decomposing biochemical from structural signals. Remote Sens. Environ. 81:355-364.

Sims, D.A., and J.A. Gamon. 2003. Estimation of vegetation water content and photosynthetic tissue area from spectral reflectance: A comparison of indices based on liquid water and chlorophyll absorption features. Remote Sens. Environ. 84:526-537.

Smart, D.R., A. Breazeale, and V. Zufferey. 2006. Physiological changes in plant hydraulics induced by partial root removal of irrigated grapevine (Vitis vinifera cv. Syrah). Am J. Enol. Vitic. 57:201-209.

Stimson, H.C., D.D. Breshears, S.L. Ustin, and S.C. Kefauver. 2005. Spectral sensing of foliar water conditions in two co-occurring conifer species: Pinus edulis and Juniperus monosperma. Remote Sens. Environ. 96:108-118.

Strachan, I.B., E. Pattey, and J.B. Boisvert. 2002. Impact of nitrogen and environmental conditions on corn as detected by hyperspectral reflectance. Remote Sens. Environ. 80:213-224.

Turner, M.T., and G.P. Jarvis. 1982. Measurement of plant water status by the pressure chamber technique. Irrig. Sci. 9:289-308.

van Niel, T.G., T.R. McVicar, H. Fang, and S. Liang. 2003. Calculating environmental moisture for per-field discrimination of rice crops. Int. J. Remote Sens. 24:885-890.

Vogelmann, J.E., B.N. Rock, and D.M. Moss. 1993. Red edge spectral measurements from sugar maple leaves. Int. J. Remote Sens. 14:1563-1575.

Williams, L.E., and F.J. Araujo. 2002. Correlations among predawn leaf, midday leaf, and midday stem water potential and their correlations with other measures of soil and plant water status in Vitis vinifera. J. Am. Soc. Hortic. Sci. 127:448-454.

Williams, L.E., and T.J. Trout. 2005. Relationships among vine- and soil-based measures of water status in a Thompson seedless vineyard in response to high-frequency drip irrigation. Am. J. Enol. Vitic. 56:357-366.

Zarco-Tejada, P.J., and S.L. Ustin. 2001. Modeling canopy water content for carbon estimates from MODIS data at land EOS validation sites. In Geoscience and Remote Sensing Symposium. IGARSS '01 Proceedings. Sydney, Australia. 1:342-344.

Zarco-Tejada, P.J., J.R. Miller, G.H. Mohammed, T.L. Noland, and P.H. Sampson. 1999. Canopy optical indices from infinite reflectance and canopy reflectance models for forest condition monitoring: Application to hyperspectral CASI data. In Geoscience and Remote Sensing Symposium. IGARSS '99 Proceedings. Hamburg, Germany. 3:1878-1881.

Zarco-Tejada, P.J., J.R. Miller, G.H. Mohammed, and T.L. Noland. 2000. Chlorophyll fluorescence effects on vegetation apparent reflectance: I. Leaf-level measurements and simulation of reflectance and transmittance spectra. Remote Sens. Environ. 74:582-595.

Zarco-Tejada, P.J., J.R. Miller, G.H. Mohammed, T.L. Noland, and P.H. Sampson. 2001. Scaling-up and model inversion methods with narrow-band optical indices for chlorophyll content estimation in closed forest canopies with hyperspectral data. IEEE Trans. Geosci. Remote Sens. 39:1491-1507.

Zarco-Tejada, P.J., C.A. Rueda, and S.L. Ustin. 2003. Water content estimation in vegetation with MODIS reflectance data and model inversion methods. Remote Sens. Environ. 85:109-124.

Zarco-Tejada, P.J., A. Berjón, R. López-Lozano, J.R. Miller, P. Martín, V. Cachorro, M.R. González, and A. de Frutos. 2005a. Assessing vineyard condition with hyperspectral indices: Leaf and canopy reflectance simulation in a row-structured discontinuous canopy. Remote Sens. Environ. 99:271-287.

Zarco-Tejada, P.J., S.L. Ustin, and M.L. Whiting. 2005b. Temporal and spatial relationships between within-field yield variability in cotton and high-spatial hyperspectral remote sensing imagery. Agron. J. 97:641-653.

Zhao, D.H., J.L. Li, and J.G. Qi. 2005. Identification of red and NIR spectral regions and vegetative indices for discrimination of cotton nitrogen stress and growth stage. Comput. Electron. Agric. 48:155-169.